Electrochemical removal of phenol in alkaline solution. Contribution of the anodic polymerization on different electrode materials

Noureddine Belhadj Tahar[a], André Savall[b,*]

[a] *Département de Chimie, Faculté des Sciences de Monastir, Université de Monastir, Route de Kairouan, 5000 Monastir, Tunisia*
[b] *Laboratoire de Génie Chimique, CNRS, Université Paul Sabatier, 118, Route de Narbonne, 31062 Toulouse cedex 9, France*

A B S T R A C T

The removal of organic pollutants based on electropolymerization on an anode was performed in the case of phenol in alkaline solution. The polymer formed by a process involving less than two electrons per molecule of phenol, is then precipitated by decreasing the pH and finally filtered and disposed. The electrochemical polymerization of phenol (C_0 = 0.105 M) in alkaline solution (pH = 13) at 86 °C has been studied by galvanostatic electrolysis, using a range of anode materials characterized by different O_2-overpotentials (IrO_2, Pt and β-PbO_2). Measurements of total organic carbon and HPLC have been used to follow phenol oxidation; the morphology of the polymer deposited on the electrode surface has been examined by SEM. Experimental data indicate that phenol concentration decreases by oxidation according to a first order reaction suggesting a mass transport limitation process. Polymeric films formed in alkaline solution did not cause the complete deactivation of the anodes. SEM results show that the polymeric films formed on Ti/IrO_2 and Pt anodes cannot be mineralized. On the other hand, complex oxidation reactions leading to the partial incineration of polymeric materials can take place on the Ta/β-PbO_2 surface due to electrogenerated HO• radicals which have an oxidizing power much higher than that of intermediaries formed respectively on IrO_2 and Pt. It is assumed that the polymer films formed on these anodes have different permeability characteristics which determine the rate of mass transfer of the phenol. The fractions of phenol converted in polymers were 25, 32 and 39% respectively with Ti/IrO_2, Pt and Ta/β-PbO_2, a series of materials in which the O_2-overvoltage increases.

1. Introduction

Electrochemical oxidation has been proposed as an efficient method for the treatment of wastewater polluted by organics since mineralization of organic pollutants can be completely achieved at different anode materials: SnO_2 [1–6], PbO_2 [1,7–12] and boron doped diamond (BDD) [13–17]. BDD is considered as a promising material; however, BDD electrodes are still under development in view to increase their robustness and to reduce fabrication costs of equipments [17]. In wastewater treatment the removal of phenols is of great importance due to their toxicity [10]. Destruction of phenols by electrochemical oxidation has been investigated intensively; however, this technique of mineralization suffers from low reaction rates and low current efficiencies [18,19]. The main reason for the low oxidation rate is electrode fouling. Phenols are well known for their ability to foul anodes; the tarry deposit is attributed to anodic polymerization [20]. Electropolymerization of phenols has been studied on different electrodes such as Au [21], glassy carbon [20], Pt [4,5,22–25], PbO_2 [26] and BDD [13,14]. From these investigations a global mechanism is commonly accepted for electropolymerization of phenol [21,22,27–30]; at pH value higher than phenol pK_a (9.89), phenate anion gives rise, during the first step of oxidation, to phenoxy radical:

$$C_6H_5O^- \rightarrow C_6H_5O^\bullet + 1e^- \quad (1)$$

A phenoxy radical can react irreversibly with an other radical or with an unreacted phenate anion via C–C or C–O coupling to form dimeric products [5,19,22,24,29–34]. For example:

$$2C_6H_5O^\bullet \xrightarrow{C-C\ Coupling} \underset{Dimer}{HOC_6H_4C_6H_4OH} \quad (2)$$

$$2C_6H_5O^\bullet \xrightarrow{C-O\ Coupling} \underset{Dimer}{C_6H_5OC_6H_4OH} \quad (3)$$

Such dimer can be oxidized again to produce a new radical which can couple with a phenoxy radical or with other dimeric radical to produce the polymer. For example:

$$C_6H_5OC_6H_4OH \xrightarrow{-e^-,-H^+} C_6H_5OC_6H_4O^\bullet \quad (4)$$

* Corresponding author. Tel.: +33 5 61556110; fax: +33 5 61556139.
E-mail address: savall@chimie.ups-tlse.fr (A. Savall).

$$C_6H_5OC_6H_4O^{\bullet} \xrightarrow[-(n-1)e^-,-(n-1)H^+]{^{n}C_6H_5O^{\bullet}} \underset{\text{Polymer}}{C_6H_5O[C_6H_4O]_nC_6H_4OH} \quad (5)$$

Gattrell and Kirk [20,35] reported that tars formed by electropolymerization of phenol show low permeability and strong adhesion to the electrode. The formation rate of tars depends on phenoxy radical concentration which can be limited by decreasing the concentration of phenol. This film was considered to be composed of (i) a tightly adsorbed layer of products of oxidation and polymerization covered with (ii) polymeric and oligomeric layers [36,37]. The tightly adsorbed layer is unaffected by oxygen evolution while the upper layers can be disrupted by gas evolution. Therefore, oxygen evolution is beneficial to prevent complete deactivation of the electrode by a thick polymeric film; however, electron transfer remains hindered by a barrier at the electrode surface.

Many phenols have been oxidized on anode materials having high oxygen overpotentials such as PbO_2 [38] and BDD [13,14,38]. It is now generally assumed that, in the potential region of water decomposition, mineralization of organics occurs by transfer of oxygen atoms from the active electrogenerated hydroxyl radicals (Reaction (6)):

$$H_2O \xrightarrow{-e^-,-H^+} HO^{\bullet} \quad (6)$$

Thus, the polymeric film can be oxidized by hydroxyl radicals as soon as its formation at the electrode surface that prevents fouling. The aim of these works was the efficient mineralization of organic pollutants thanks to high oxidizing power of hydroxyl radicals. However, low current yields are caused by the concurrent reaction of oxygen evolution:

$$2HO^{\bullet} \xrightarrow{-2e^-,-2H^+} O_2 \quad (7)$$

On the other hand, formation of polymer, occurring by direct electron transfer in the potential region of water stability, could be convenient in wastewater treatment with respect to energy consumption since less than two electrons is required per phenol molecule to trigger polymerization [29,33]. The removal of some phenolic compounds from aqueous solutions based on electropolymerization was recently attempted [33,39–41]. By this method phenol is immobilized as a solid polymer on the anode surface by electrolysis at a low anodic current density in neutral solution. Gattrel et al. and Kuramitz et al. have used as anodes respectively a granular activated carbon [33] and a bundle of carbon fiber [39–41] having large surface area to remove successfully phenols from very diluted solutions. This method represents a simple and clean technique for the complete removal of phenolic compounds in aqueous solution. However, after use, the carbon fiber and the granular activated carbon passiveted by the film of polymer must be regenerated. Zareie et al. [42] have shown that the removal of phenol from wastewater in the form of a solid polymer suspended in the reactor can be achieved using a carbon electrode and high anodic current density in the presence of NaCl ($120\,g\,l^{-1}$); these authors suggested that most of the phenol oxidation occurs in the solution bulk without electrode fouling. One can object that this process uses a large amount of salt and would form toxic organohalogeno compounds.

In a previous work [26], we underlined that electropolymerization of phenol could help to improve the efficiency in wastewater treatment. The effects of initial phenol concentration, anodic current density, pH and process temperature on phenol oxidation were studied using a Ta/β-PbO_2 anode in batch runs. It has been shown that 15% of the starting phenol can be removed as polymers under the best operating conditions. In our knowledge, the direct quantification of phenol conversion into polymer as a suspension in the electrolytic solution was not the object of any study. It was also shown that the fraction of starting phenol converted into polymer increases substantially with temperature from 25 to 65 °C [26]. Gattrell and Kirk [20] have also observed during electrolysis of phenol in sulphuric acid aqueous solution on Pt that electrode passivation was reduced or prevented by increasing temperature.

The efficiency of phenol removal by electropolymerization is strictly related to the operating conditions and the nature of the anode material. The aim of the present work is to investigate and to compare the efficiency of three electrode materials (IrO_2, Pt and β-PbO_2), which have different oxygen overpotentials, for removal of phenol in aqueous solution by electropolymerization. Furthermore, the effect of the nature of the substrate (Ta or Nb) used for the electrodeposition of β-PbO_2 on the electropolymerization of phenol was tested. Batch runs were carried out, using these anodes, in alkaline media ($pH > pK_a$) in view to increase the solubility of polymers and therefore to reduce fouling. As the effect of varying temperature from 25 to 65 °C was previously found to be a positive fact [26], all the experiments were conducted at a temperature equal to 86 °C.

Table 1
Experimental conditions for β-PbO_2 electrodeposition. 1 M $Pb(NO_3)_2$; temperature: 65 °C; electrodeposition time for each current density value: 30 min.

Substrate	J ($mA\,cm^{-2}$)	Nature of deposit
Tantalum	100	Adherent, rough, with many big pinholes, mat and grey in color.
Niobium	100	Adherent, smooth, uniform, without pinholes, mat and grey in color.

2. Experimental

2.1. Preparation of β-PbO_2 anode

β-PbO_2 deposits were electrochemically prepared on rectangular plates of massive niobium or tantalum (70 mm × 10 mm × 1 mm) from lead nitrate solution. Tantalum and niobium have very good chemical and electrochemical stability. β-PbO_2 was deposited on these substrates by anodic oxidation of lead nitrate solution at low anodic current density [43–45].

2.1.1. Surface treatment

Tantalum and niobium plates were sandblasted and then etched. The losses in mass per unit of surface area due to this surface treatment were 0.73 ± 0.12 and $0.44 \pm 0.08\,mg\,cm^{-2}$ respectively for tantalum and niobium plates. More details on the surface treatment procedure are given in our previous work [9,26].

2.1.2. Anodic deposition of β-PbO_2

Pure β-PbO_2 was obtained by electrolysis of $Pb(NO_3)_2$ solutions using anodic constant current densities higher than $100\,mA\,cm^{-2}$. The deposition procedure was previously described [9,26]; the operating conditions are summarized in Table 1.

2.2. Preparation of Ti/IrO_2

Conductive metal oxide IrO_2 was deposited on a titanium substrate (70 mm × 10 mm × 1 mm) by the thermal decomposition technique [46,47].

2.2.1. Surface treatment

Titanium substrate underwent the same mechanical surface treatment as tantalum and niobium ones. The average loss in mass was $0.16 \pm 0.05\,mg\,cm^{-2}$. Chemical etching was then carried out using boiling concentrated hydrochloric acid (32% by mass)

Table 2
Effect of the anode nature on the electrochemical polymerization of phenol. Initial phenol concentration: 105 mM; current density: 200 mA cm^{-2}; temperature: 86 °C and pH 13. Q is the electrical charge passed during electrolysis at the complete disappearance of phenol.

Electrode	Q (Ah l^{-1})	r(polymers) (%)	r(aromatics) (%)	r(aliphatics) (%)	r(CO_2) (%)	r(quantified products) (%)	$k_{app.}$ (h^{-1})	$k_m \times 10^5$ (m s^{-1})	CE (%)
Ti/IrO_2	200	25	9	8	38	80	0.42	0.8	24
Pt	120	32	18	6	19	75	0.66	1.3	22
Ta/β-PbO_2	60	39	14	19	4	76	2.20	4.3	16

for 30 min. The loss in mass due to this chemical treatment was 13.07 ± 1.85 mg cm^{-2}.

2.2.2. Deposition of a layer of IrO_2 by thermal treatment

The etched titanium substrate was then covered with an insoluble and electrically conductive metal oxide IrO_2 obtained by thermal decomposition of hexachloroiridic acid dissolved in 2-propanol. The solution was firstly prepared by dissolving 480 mg of H_2IrCl_6, $6H_2O$ in 5 ml of isopropanol. This solution was brushed onto the titanium substrate then the solvent was evaporated at 60 °C. The electrode was then submitted to a thermal treatment at 530 °C in air atmosphere during 10 min and then cooled. This operation sequence (painting, evaporation and thermal treatment) was repeated 10 times. The final stage consisted of heating in air to 530 °C for 2 h. The average mass of iridium oxide deposited per unit of surface area was 0.65 ± 0.07 mg cm^{-2}.

2.3. Platinum anode

The platinum (Good fellow PT007950, 99.95%) anode was a rod (ϕ = 5 mm, L = 10 cm).

2.4. Electrolyses

Electrolyses of phenol aqueous solutions (V_0 = 140 ml) were carried out in a two-compartment cylindrical reactor, at constant temperature of 86 °C, under magnetic stirring. The electrolytic solutions initially contained only phenol at a concentration of 105 mM. The initial pH was adjusted to 13, before and over electrolyses, by adding sodium hydroxide solution at 5 M. The cathode was a graphite rod (ϕ = 1 cm; L = 6 cm) placed in a porous ceramic cylinder (Norton, RA 84) containing a 1 M sulphuric acid solution. The working area S of the anode was 20 cm^2. The phenol aqueous solutions were electrolysed galvanostatically under an anodic current density of 200 mA cm^{-2}.

All electrolyses were carried out until the practical disappearance of the starting phenol. It was assumed that phenol was completely oxidized when its concentration in the solution reached a value lower than 0.1 mmole dm^{-3}; this limit defined the electrolysis time and the electrical charge values Q presented in Tables 2 and 3. These values of the charge depend on the operating conditions (see Fig. 2).

2.5. Voltamperometry

Cyclic voltammetry and chronoamperometry measurements were carried out in a conventional three-electrode cell (200 ml) using a computer controlled Eco Chemie Autolab Model 30 (Utrecht, The Netherlands). The working electrode was a vitreous carbon disk with a geometric area of 0.0707 cm^2. The counter and reference electrodes were respectively platinum spiral and $Hg/Hg_2Cl_2/Cl^-$ (sat.). Before each experiment, the working electrode was polished to a mirror with 1 μm alumina slurries on polishing sheet (3 M 262X IMPERIAL Lapping Film) and subsequently washed with distilled water.

Cyclic voltammetry was performed in aqueous solution containing 1 M sodium hydroxide and 10 mM phenol.

2.6. Analyses

2.6.1. High performance liquid chromatography

Analyses of phenol and of its main oxidation intermediate products were carried out by liquid chromatography using a Hewlett Packard 1090 HPLC apparatus. Phenol and its oxidation products were separated thanks to a Hamilton PRP X 300 column and quantified by measurement of optical density at 220 nm at the column output using a diode array detector. Experimental details were given in our previous works [9,26].

2.6.2. Total organic carbon (TOC)

TOC was measured using a Model 700 TOC Analyser (purchased from O. I Analytical). Before each analysis, the sample was appropriately diluted with a 5 M H_2SO_4 solution to make precipitate polymers and to eliminate CO_2 from carbonate. The sample was then filtrated (Millipore type GV, 0.45 μm).

2.6.3. Determination of the fraction of starting phenol converted into polymers

Polymers formed during electrolysis of aqueous solution containing 0.105 M phenol and 0.1 M NaOH are soluble which is in agreement with Grace's patent [48]. The polymers precipitated in the form of black particles by addition of 5 M sulphuric acid to the solution (around 12 ml per litre). The solid polymers were subsequently separated (Millipore type GV, 0.45 μm) and dissolved in a sodium hydroxide solution at 1 M (V = 1 l). HPLC analyses have confirmed that these alkaline solutions were free of aromatic or aliphatic intermediates of phenol oxidation; the chromatogram presents a broad peak attributed to polymers but no peak corresponding to any one of the phenol oxidation intermediates. Furthermore, comparison between the UV–vis spectrum of polymer and those of phenol, 1,4-benzoquinone and maleic acid showed that neither phenol nor its main oxidation products precipitated after addition of 5 M sulphuric acid to the electrolysed solution (Fig. 1). Indeed, Fig. 1B shows that phenol, 1,4-benzoquinone and maleic acid absorb in the same wavelength range (≤300 nm) while a long tail grows at higher wavelength (≥300 nm) in the case of polymers Fig. 1A.

Table 3
Effect of the substrate nature used for β-PbO_2 electrodeposition on the performance in phenol electropolymerization. Same conditions as in Table 2.

Electrode	Q (Ah l^{-1})	r(polymers) (%)	r(aromatics) (%)	r(aliphatics) (%)	r(CO_2) (%)	r(quantified products) (%)	$k_{app.}$ (h^{-1})	$k_m \times 10^5$ (m s^{-1})	CE (%)
Ta/β-PbO_2	60	39	14	19	4	76	2.20	4.3	16
Nb/β-PbO_2	120	24	23	17	21	85	0.69	1.3	36

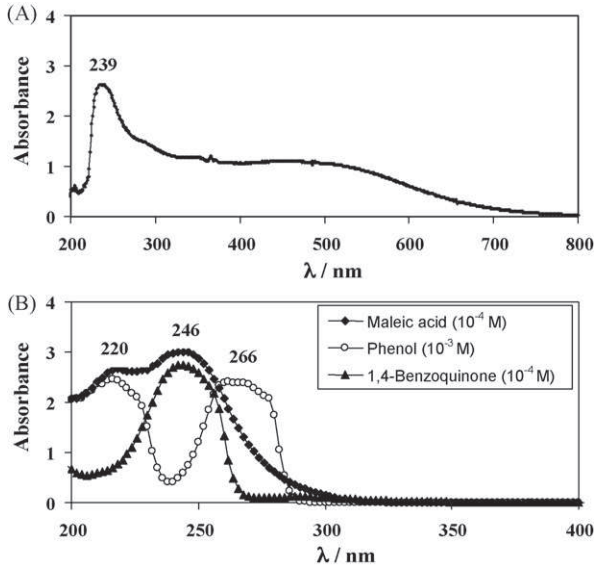

Fig. 1. UV–vis spectra of polymer in 1 M NaOH aqueous solution (A) and phenol, 1,4-benzoquinone and maleic acid in aqueous solution (B).

The fractions of starting phenol converted respectively into polymers, aromatics, aliphatics, and carbon dioxide were defined as follows:

$$r(\text{polymers}) = \frac{[\text{TOC}]_2 \times V}{[\text{TOC}]_0 \times V_0} \times 100 \quad (8)$$

$$r(\text{aromatics}) = \frac{[\text{aromatics}]}{[\text{C}_6\text{H}_5\text{OH}]_0} \times 100 \quad (9)$$

$$r(\text{aliphatics}) = \frac{[\text{aliphatics}]}{[\text{C}_6\text{H}_5\text{OH}]_0} \times 100 \quad (10)$$

$$r(\text{CO}_2) = \frac{[\text{TOC}]_0 - [\text{TOC}]_1}{[\text{TOC}]_0} \times 100 - r(\text{polymers}) \quad (11)$$

where $[\text{TOC}]_0$ is the total organic carbon of the phenol solution before electrolysis (g l^{-1}), $[\text{TOC}]_1$ is the total organic carbon of the phenol solution after electrolysis and filtration of polymers (g l^{-1}), $[\text{TOC}]_2$ is the total organic carbon of the sodium hydroxide solution in which polymers were dissolved (g l^{-1}), V_0 and V are respectively the volumes of the electrolysed solution and of the sodium hydroxide solution in which polymers were dissolved (l). [aromatics] and [aliphatics] are the concentrations of respectively aromatic (hydroquinone (HQ), catechol (Cat) and 1,4-benzoquinone (BQ)) and aliphatic (maleic (MA) and fumaric (FA) acids) intermediates (M) and $[\text{C}_6\text{H}_5\text{OH}]_0$ is the initial phenol concentration (M); all these concentrations were monitored by HPLC measurements.

The fraction of quantified products relative to the starting phenol was defined as follows:

$$r(\text{quantified products}) = r(\text{polymers}) + r(\text{aromatics}) + r(\text{aliphatics}) + r(\text{CO}_2) \quad (12)$$

The electrical charge $Q_{\text{tot.}}$ (C) used to form all the intermediate products in the proportions found by HPLC and TOC measurements (polymers and carbon dioxide) can be calculated by:

$$Q_{\text{tot.}} = FV_0\{2([\text{HQ}] + [\text{Cat}]) + 4[\text{BQ}] + 8([\text{MA}] + [\text{FA}])\} + F\left\{28\left(\frac{([\text{TOC}]_0 - [\text{TOC}]_1)V_0 - [\text{TOC}]_2 V}{6 \times 12}\right) + \frac{[\text{TOC}]_2 V}{6 \times 12}\right\} \quad (13)$$

In this expression, the terms $(([\text{TOC}]_0 - [\text{TOC}]_1)V_0 - [\text{TOC}]_2 V/(6 \times 12))$ and $[\text{TOC}]_2 V/(6 \times 12)$ represent the mole number of phenol converted respectively into CO_2 and polymers. The charge involved in the formation of polymers is calculated on the basis of an exchange of one electron per phenol molecule.

The current efficiency (CE), expressed as a percentage, was defined as:

$$\text{CE} = \frac{Q_{\text{tot.}}}{I \times t} \times 100 \quad (14)$$

where I was the current applied during the electrolysis (A) and t the electrolysis time (s).

Values of r(polymers), r(aromatics), r(aliphatics), $r(\text{CO}_2)$, Q and CE, presented in Table 2, were calculated at electrolysis times corresponding to the complete disappearance of the starting phenol from solutions.

Carbon dioxide formed during electrolysis was absorbed in the alkaline solution to form carbonates and addition of sulphuric acid (5 M) to the final solution leaded to a strong carbon dioxide evolution.

2.6.4. Scanning electron microscope (SEM)

After electrolysis, a plate of Ta/β-PbO_2 and an other plate of Ti/IrO_2 were rinsed with distilled water and then dried. Furthermore, second plates of each one of these electrodes were plunged for 30 min in 1 M sodium hydroxide aqueous solution in view to completely eliminate the polymeric films remaining on their surface. Then, these plates were rinsed with distilled water and dried. The surface of the stripped plate had a slightly different shade compared to that of the unstripped one, easily observable to the naked eye. A SEM analysis was performed on both the stripped and unstripped plates. The scanning electron micrographs were obtained with a JSM 6700F NT microscope.

3. Results and discussion

3.1. Oxidation products of phenol

The main products formed during anodic oxidation of aqueous solutions of phenol are hydroquinone, catechol, 1,4-benzoquinone, maleic acid, fumaric acid, carbon dioxide and polymers [9,26]. For all electrolyses carried out in the present work, the percentage of quantified products was at around 80% (Tables 2 and 3). The remaining 20% were in the form of aliphatic carboxylic acids of lower molecular weights, not quantified by HPLC, and oligomers or polymers deposited on the anode surface in reason of the local acidity (Eqs. (6) and (7)). Indeed, the concentration of protons $[\text{H}^+]_{\text{elec.}}$ on the anode surface, where water discharge takes place (Eq. (6)), can be correlated to the current density ($2000\ \text{A m}^{-2}$) by the following equation: $i = nFk_{\text{H}^+}[\text{H}^+]_{\text{elec.}}$ considering that the bulk concentration of protons is equal to zero owing to the high pH value (pH = 13). The concentration of H^+ at the electrode surface, $[\text{H}^+]_{\text{elec.}}$, is equal to around 1 M for $n = 2$ and the mass transfer coefficient $k_{\text{H}^+} = 10^{-5}\ \text{m s}^{-1}$; this high value could explain the formation of an insoluble and adherent film of polymer on the anode surface.

For all electrolyses performed in this work, the decrease of phenol concentration with time (Fig. 2) follows a kinetic law corresponding to a first-order reaction described by Eq. (15):

$$\ln\frac{[\text{C}_6\text{H}_5\text{OH}]_0}{[\text{C}_6\text{H}_5\text{OH}]_t} = k_{\text{app.}} \times t \quad (15)$$

where $[\text{C}_6\text{H}_5\text{OH}]_t$ is the phenol concentration (M) at time t and $k_{\text{app.}}$ is the apparent rate constant. The term apparent specifies that diffusion of phenol occurs through the liquid diffusion layer and the layer of polymers and/or oligomers deposited on the electrode.

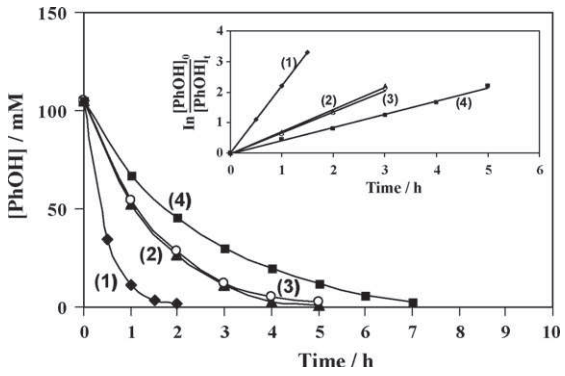

Fig. 2. Decrease of phenol concentration during electrolyses of phenol aqueous solutions (105 mM) at a constant current density of 200 mA cm^{-2} and a temperature of 86 °C on different anode materials. Inset: linear regression for phenol disappearance with time. (1) Ta/β-PbO_2, (2) Nb/β-PbO_2, (3) Pt and (4) Ti/IrO_2.

Eq. (15) has the typical form of an electrochemical process limited by diffusion in which:

$$k_{app.} = \frac{k_m \times S}{V_0} \tag{16}$$

where S is the working area of the anode and V_0 is the volume of the solution. For a process strictly limited by diffusion, k_m is the overall mass-transfer coefficient.

3.2. Influence of the anode material nature

Our main objective was to find conditions which favour electropolymerization of phenol and avoid (i) anode fouling by forming a dense film with a low permeability and (ii) mineralization of the phenol. In this frame, the electrochemical polymerization of phenol has been investigated at several anodic materials. Electrolyses of alkaline solutions of phenol were carried out, under the same operating conditions using Ti/IrO_2, Pt and Ta/β-PbO_2 anodes. Experimental results show that the rate constant $k_{app.}$ (Table 2) depends strongly on the nature of the anode material used. The rate values of the phenol concentration decrease are in the order: Ta/β-PbO_2 > Pt > Ti/IrO_2; phenol disappears completely after passing a charge Q of 60, 120 and 200 Ah l^{-1} respectively for Ta/β-PbO_2, Pt and Ti/IrO_2. Similar results have been reported by Rodgers et al. [49]; these authors found that the rate of disappearance of phenol was around 4.3 faster at Pb/PbO_2 than at Ti/IrO_2. Table 2 shows that the fraction of starting phenol converted into polymers increases according to the nature of the anode material as follows: Ti/IrO_2 < Pt < Ta/β-PbO_2. With Ta/β-PbO_2 anode it is possible to convert around 40% of the starting phenol into polymers; these polymers can be extracted from the solution by simple filtration after acidification. In our previous work [26], under the same operating conditions but at lower temperature (25–65 °C), the maximum value of this conversion was only 15% at 65 °C. This effect of the temperature will be explained in Section 3.4.

It is of interest to note that the higher is the amount of polymer formed the lower is the fraction of starting phenol converted into CO_2 (Table 2). Current efficiency values, calculated by Eq. (14) at the complete disappearance of phenol from solution were around 20% for the three electrodes. In fact, the current efficiency could be improved by using lower experimental anodic current density. Indeed, the limiting current density for phenol oxidation, calculated by equation: $i_{lim.} = nFk_m[PhOH]_0$, is equal to around 200 A m^{-2} for $n = 2$, $k_m = 10^{-5}$ m s^{-1} (see Table 2) and $[PhOH]_0 = 105$ mol m^{-3}. The experimental current density (2000 A m^{-2}) was quite higher than the limiting current density. We have chosen this high current density in view to compare the three anodes tested in the oxygen evolution region with similar conditions of the attacking of oxygen bubbles onto the polymeric film. Work is in progress to optimize the value of the anodic current density.

Although electrolyses were carried out in alkaline medium in which polymers are soluble, solid black particles precipitated on the

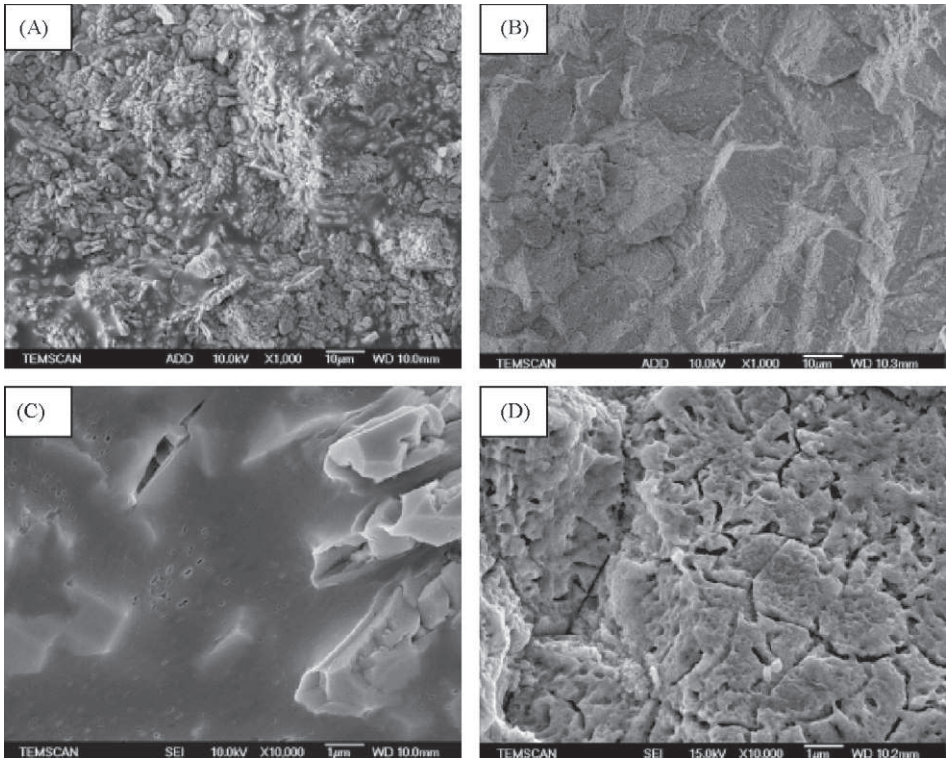

Fig. 3. Scanning electron micrographs of Ta/β-PbO_2 anode used in electrolysis of phenol aqueous solution. (A, C) before and (B, D) after chemical stripping for 30 min in 1 M NaOH aqueous solution. C and D micrographs are at 10 times the magnification shown in A and B.

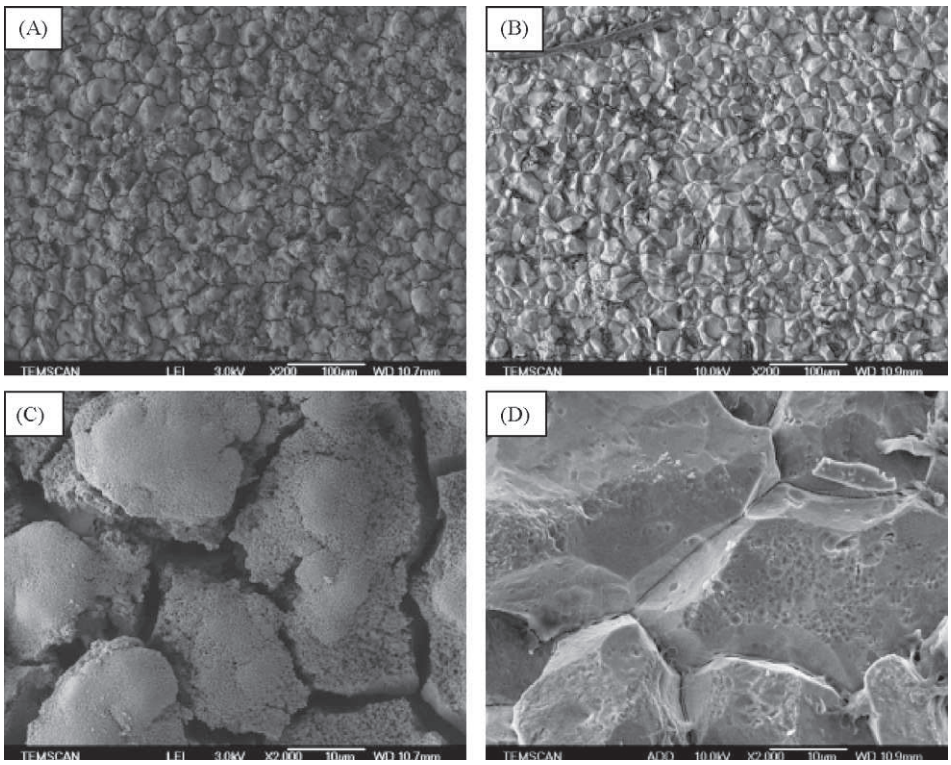

Fig. 4. Scanning electron micrographs of Ti/IrO_2 anode used in electrolysis of phenol aqueous solution. (A, C) before and (B, D) after chemical stripping during 30 min in 1 M NaOH aqueous solution. C and D micrographs are at 10 times the magnification shown in A and B.

$Ta/\beta\text{-}PbO_2$ anode surface and were visible to the naked eye. The film of polymers formed on the Ti/IrO_2 anode was homogeneous thin and adherent. Although homogeneous and adherent, the polymeric films formed on Pt were thick (thickness of around 1 mm).

Fig. 3 shows SEM micrographs of the unstripped (Fig. 3A and C) and stripped (Fig. 3B and D) $Ta/\beta\text{-}PbO_2$ electrode surface. The adherent and stable polymeric film was present only in certain places on the $Ta/\beta\text{-}PbO_2$ surface. Fig. 4 shows that, contrary to $Ta/\beta\text{-}PbO_2$, the

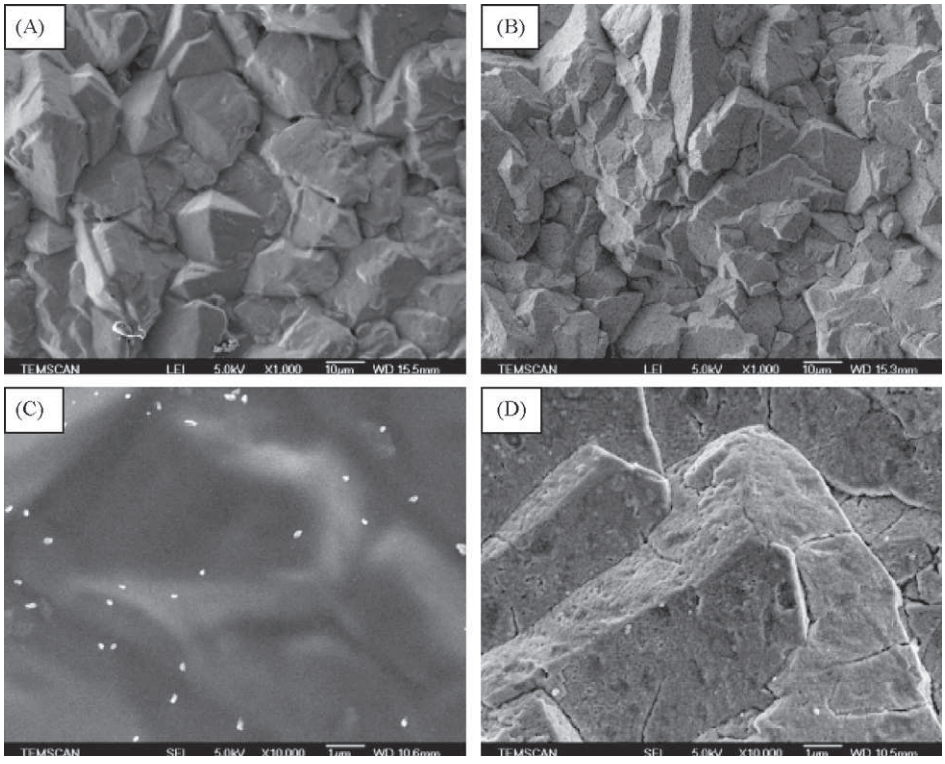

Fig. 5. Scanning electron micrographs of $Nb/\beta\text{-}PbO_2$ anode used in electrolysis of phenol aqueous solution. (A, C) before and (B, D) after chemical stripping during 30 min in 1 M NaOH aqueous solution. C and D micrographs are at 10 times the magnification shown in A and B.

surface of the Ti/IrO_2 anode was completely covered by an adherent polymeric film.

In spite of the deposition of a polymeric adhesive film on the electrode surface, the Ta/β-PbO_2 anode was not deactivated. Furthermore, the cell tension ΔE varied slightly from beginning (6.5 V) to the end (6.8 V) of electrolysis for all the anodes tested. This result proves that the film of polymer was hydrophilic and permeable to phenol and water.

3.3. Influence of the nature of the substrate

Values of constants $k_{app.}$ and k_m presented in Table 3 show that phenol oxidized more rapidly on Ta/β-PbO_2 than Nb/β-PbO_2; the charges Q corresponding to the complete elimination of phenol were 60 and 120 Ah l^{-1} respectively for Ta/β-PbO_2 and Nb/β-PbO_2. On the other hand, Table 3 shows that the fraction of starting phenol converted into polymers was higher with Ta/β-PbO_2 than with Nb/β-PbO_2. However, degradation of phenol into CO_2 was more promoted on Nb/β-PbO_2 than on Ta/β-PbO_2 and global current efficiencies were 16 and 36% respectively for Ta/β-PbO_2 and Nb/β-PbO_2.

SEM micrographs (Fig. 5) show that the Nb/β-PbO_2 surface was completely covered by an adherent polymeric film. The surface roughness of Ta/β-PbO_2 was greater than that of Nb/β-PbO_2 (Figs. 3 and 5).

3.4. Discussion

Reactions (1)–(5) show that any increase in phenate diffusion flux and/or generation rate of phenoxy radicals increases the polymerization rate. Under conditions of limitation by diffusion through the electrolytic solution and the polymeric film deposited on the anode surface, operating at a high anodic current density (2000 A m^{-2}) with respect to the limiting current density (200 A m^{-2}) may increase the contribution of indirect oxidation via reactive species arising from water oxidation to the detriment of direct electron transfer. The difference in reactivity of the polymer film towards its electrooxidation on Ti/IrO_2, Pt and Ta/β-PbO_2 anodes, under the same other operating conditions, results from the difference in oxidizing power of the reactive species electrogenerated from water oxidation.

It has been shown that hydroxyl radicals arisen from water oxidation are accumulated at PbO_2 anode surface [50] contrary to IrO_2 and Pt anodes for which the surface hydroxyl radical concentration is almost zero [2]. At IrO_2 anode, hydroxyl radicals interact with the oxide anode forming the higher oxide IrO_3 considered as the active specie for oxidation of phenol at IrO_2 [2,51–54]. At Pt anode, hydroperoxyl radicals ($HOO^{\bullet}$) generated from oxidation of water [50] are supposed to be the active species in phenol oxidation on Pt. The oxidizing power of these reactive species generated from oxidation of water increases as follows: $IrO_3 < HOO^{\bullet} < HO^{\bullet}$ [51,55–57]. Hydroxyl radicals, electrogenerated on Ta/β-PbO_2, are extremely reactive producing unselective oxidation [2,5,9] while selective oxidation occurs on IrO_2 which involves the IrO_3/IrO_2 couple [2].

Panizza and Cerisola have reported that hydroxyl radicals $HO^{\bullet}$ formed on lead dioxide are able to mineralize the polymeric film deposited on its surface [31]. As illustrated by Fig. 3, the polymeric film deposited on the electrode surface was oxidized; as a result of this attack the permeability of the film should increase; thus, the resistance against phenol diffusion through the film is lowered. It results that the mass transfer coefficient k_m is around 4 times higher than that observed for the IrO_2 and Pt electrodes (Table 2). Species like IrO_3 and $HOO^{\bullet}$ cannot oxidize the polymeric films formed respectively on Ti/IrO_2 (Fig. 4) and Pt. The more pronounced deactivation of Ti/IrO_2 compared to Pt may be explained by different structures (permeability to phenol molecules) of the

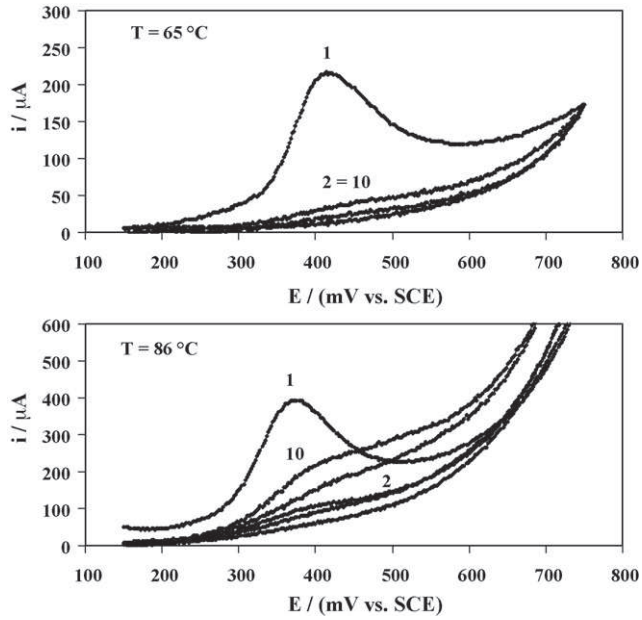

Fig. 6. Cyclic voltammograms recorded between 150 and 750 mV vs. SCE on vitreous carbon electrode for phenol 10 mM in 1 M NaOH aqueous solution at temperatures 65 and 86 °C. (1) first cycle; (2) second cycle (10) tenth cycle. Scan rate: 100 mV s^{-1}.

corresponding polymeric films; indeed, it has been reported that the polymeric film formed from phenol on Pt anode is irregular and blistered [58] and shows porous characteristics [59]. On the other hand, Fig. 4 shows that the polymeric film formed on Ti/IrO_2 surface is non-porous, regular, uniform and dense. Similar results were reported by Wang et al. [60] when they studied the oxidation of 4-chlorophenol in aqueous solution on Ti/IrO_2. These authors assumed that deactivated Ti/IrO_2 cannot be reactivated by anodic polarisation even at very high potential (2 V vs. SCE). Table 2 shows that the mass transfer coefficient (k_m), and consequently the flux of phenol, increased with the nature of the anode materials as follows: Ti/IrO_2 < Pt < Ta/β-PbO_2. When the flux of phenol at the anode surface increases, phenoxy radical concentration increases resulting in greater polymer yield (Table 2). However, these films did not affect the oxidation of water (Reaction (6)) since the cell voltage remained almost constant during electrolysis; the polymer film did not introduce an appreciable ohmic drop.

Cyclic voltammetry was used in order to explain the substantial increase of the fraction of phenol converted into polymer when the temperature was increased from 65 °C (15%) [26] to 85 °C (39%). Fig. 6 shows successive scans recorded between 150 and 750 mV vs. SCE (in the potential region of water stability) on vitreous carbon electrode for phenol 10 mM in 1 M NaOH aqueous solution at 65 and 86 °C. Fig. 6 shows that electrode passivation occurred after the first cycle at both 65 and 85 °C; indeed, no phenol oxidation peak was observed right from the second cycle. Visual examination of the electrode surface revealed the presence of adherent films of polymer. At the temperature of 85 °C and after the second cycle, the phenol oxidation was expressed as a wave which progressively increased until the tenth scan (Fig. 6). On the contrary, at 65 °C, a steady state corresponding to the complete electrode passivation was obtained as soon as the second cycle (Fig. 6). These experimental results indicate that the polymer films formed at 65 and 85 °C have different permeability characteristics. We assumed that polymers formed at high temperature (85 °C) have a high permeability which makes easier phenol diffusion towards the electrode surface, while those formed at lower temperature present a lower permeability (dense film), which slow down phenol diffusion; we have shown that lower temperatures favour mineralization of the

organic matter on a PbO_2 anode [26]. Although polymers have a higher permeability at 85 °C, they slow down nevertheless the diffusion of phenol; the peak of oxidation is then transformed into a wave and the potential moves from 380 mV (scan 1) towards 400 mV (scan 10). The influence of temperature on the electrode passivation in alkaline solution containing phenol has been particularly studied in [61].

Table 3 shows that Ta/β-PbO_2 is more efficient than Nb/β-PbO_2 if we consider the fraction of starting phenol converted into polymers. The difference could be interpreted by considering the surface morphology of β-PbO_2 deposits on the two substrates. On Ta, the β-PbO_2 deposit is very porous and presents a high roughness while that deposited on Nb is smooth and does not present pinholes (Table 1). We think that, during phenol electrolysis, oxygen evolution occurring within the porous Ta/β-PbO_2 deposit can mechanically remove the polymeric film that prevents it to adhere on the anode surface. On the other hand, Lormeau et al. [44] have shown by X-ray analysis that lead dioxide has a chemical composition depending on the substrate (Nb or Ta). Thus, hydroxyl radicals may be more weakly adsorbed on Ta/β-PbO_2 than on Nb/β-PbO_2; consequently, Ta/β-PbO_2 can be more reactive towards the polymeric film. As a result, the film forms only on certain areas on Ta/β-PbO_2 (Fig. 3). On the contrary, the polymeric film formed on the Nb/β-PbO_2 anode (Fig. 4) was tightly adsorbed and unaffected by oxygen evolution. This film has the possibility of retarding diffusion kinetics of phenol as illustrated by the low value of k_m obtained with Nb/β-PbO_2 compared to that obtained with Ta/β-PbO_2 (Table 3). Therefore, as might be expected, lower phenol flux gives lower concentration of phenoxy radicals near the anode of Nb/β-PbO_2 and so smaller amount of polymers (Table 3). As a consequence of the slowing down of the diffusion flux of phenol induced by the polymeric film on Nb/β-PbO_2, phenol oxidation tends to be complete into CO_2 (Table 3).

It should be further interesting to test the lead dioxide-coated titanium anode as candidate for industrial use in reason of its robustness and long service life [62].

4. Conclusions

The decrease of phenol concentration during electrolysis shows that it oxidizes according to a first-order reaction corresponding to limitation by diffusion. During electrochemical oxidation of phenol in alkaline aqueous solution, polymer films form on IrO_2, Pt and β-PbO_2 anodes. Polymer film grown on Ta/β-PbO_2 is not as passivating as those formed on Ti/IrO_2 and Pt. Hydroxyl radicals $HO^{\bullet}$ oxidize the polymer film formed on Ta/β-PbO_2 while IrO_3 and $HOO^{\bullet}$ cannot respectively oxidize the polymer films formed on Ti/IrO_2 and Pt. Quite different behaviours are observed for films grown on Ti/IrO_2 and Pt; thick and porous (permeable) film was formed on Pt while thin, non-porous and dense (low permeability) film was formed on Ti/IrO_2.

It is assumed that the permeability of polymers increases with a rise in temperature. The diffusion limitation of phenol depending on the permeability of the polymer films formed on the anodes used is considered as the main step which controls the phenol oxidation rate. The fractions of starting phenol converted into polymer suspended in the reactor are 25, 32 and 39% respectively for Ti/IrO_2, Pt and Ta/β-PbO_2 anodes.

Ta/β-PbO_2 is more efficient than Nb/β-PbO_2 to convert the starting phenol into polymers. In the case of Nb/β-PbO_2, a low permeable polymeric film covers completely the active surface and slows down the phenol diffusion.

This work discloses the possibility of a new way for the treatment of phenols in water based on the anodic polymerization that could improve the electrochemical treatment process.

References

[1] A.M. Polcaro, S. Palmas, F. Renoldi, M. Mascia, J. Appl. Electrochem. 29 (1999) 147.
[2] Ch. Comninellis, Electrochim. Acta 29 (1994) 1857.
[3] S. Stuki, R. Kötz, B. Carcer, W. Suter, J. Appl. Electrochem. 21 (1991) 99.
[4] Ch. Comninellis, C. Pulgarin, J. Appl. Electrochem. 23 (1993) 108.
[5] X.-Y. Li, Y.-H. Cui, Y.-J. Feng, Z.-M. Xie, J.-D. Gu, Water Res. 39 (2005) 1972.
[6] R. Kötz, S. Stuki, B. Carcer, J. Appl. Electrochem. 21 (1991) 14.
[7] F. Bonfatti, S. Ferro, F. Levezzo, M. Malacarne, G. Lodi, A. De Battisti, J. Electrochem. Soc. 146 (1999) 2175.
[8] J. Feng, L.L. Houk, D.C. Johnson, S.N. Lowery, J.J. Carey, J. Electrochem. Soc. 142 (1995) 3626.
[9] N. Belhadj Tahar, A. Savall, J. Electrochem. Soc. 145 (1998) 3427.
[10] J. Iniesta, J. Gonzalez-Garcia, E. Exposito, V. Montiel, A. Aldaz, Water Res. 35 (2001) 3291.
[11] U. Schümann, P. Gründler, Water Res. 32 (1998) 2835.
[12] Y.J. Feng, X.Y. Li, Water Res. 37 (2003) 2399.
[13] M. Panizza, P.A. Michaud, G. Cerisola, Ch. Comninellis, J. Electroanal. Chem. 507 (2001) 206.
[14] M.A. Rodrigo, P.A. Michaud, I. Duo, M. Panizza, G. Cerisola, Ch. Comninellis, J. Electrochem. Soc. 148 (2001) D60.
[15] P. Canizares, J. Garcia-Gomez, C. Saez, M.A. Rodrigo, J. Appl. Electrochem. 33 (2003) 917.
[16] G. Foti, D. Gandini, Ch. Comninellis, A. Perret, W. Haenni, Electrochem. Solid-State Lett. 2 (1999) 228.
[17] M. Fryda, Th. Matthée, S. Mulcahy, A. Hampel, L. Schäfer, I. Tröster, Diamond Relat. Mater. 12 (2003) 1950.
[18] A. Dabrowski, J. Mieluch, A. Sadkaoski, J. Wild, P. Zoltowski, Prezm. Chem. 54 (1975) 653.
[19] M. Chettiar, A.P. Watkinson, Can. J. Chem. Eng. 61 (1983) 568.
[20] M. Gattrell, D.W. Kirk, Can. J. Chem. Eng. 68 (1990) 997.
[21] J. Wang, M. Jiang, F. Lu, J. Electroanal. Chem. 444 (1998) 127.
[22] P.I. Iotov, S.V. Kalcheva, J. Electroanal. Chem. 442 (1998) 19.
[23] M. Gattrell, D.W. Kirk, J. Electrochem. Soc. 140 (1993) 903.
[24] M. Gattrell, D.W. Kirk, J. Electrochem. Soc. 140 (1993) 1534.
[25] J.-L. Boudenne, O. Cerclier, P. Bianco, J. Electrochem. Soc. 145 (1998) 2763.
[26] N. Belhadj Tahar, R. Abdelhedi, A. Savall, J. Appl. Electrochem. 39 (2009) 663.
[27] G. Mengoli, S. Daolio, M.M. Musiani, J. Appl. Electrochem. 10 (1980) 459.
[28] G. Mengoli, M.M. Musiani, Electrochim. Acta 31 (1986) 201.
[29] L. Papouchado, R.W. Sandford, G. Petrie, R.N. Adams, J. Electroanal. Chem. 65 (1975) 275.
[30] F. Bruno, M.C. Pham, J.E. Dubois, Electrochim. Acta 22 (1977) 451.
[31] M. Panizza, G. Cerisola, Electrochim. Acta 48 (2003) 3491.
[32] F.J. Vermillion, I.A. Pearl, J. Electrochem. Soc. 111 (1964) 1392.
[33] M. Gattrell, B. MacDougall, J. Electrochem. Soc. 146 (1999) 3335.
[34] Z. Ezerskis, Z. Jusys, J. Appl. Electrochem. 31 (2001) 1117.
[35] M. Gattrell, D.W. Kirk, J. Electrochem. Soc. 139 (1992) 2736.
[36] R.C. Koile, D.C. Johnson, Anal. Chem. 51 (1979) 741.
[37] M. Babai, S. Gottesfeld, Surf. Sci. 96 (1980) 461.
[38] I. Gherardini, P.A. Michaud, I. Duo, M. Panizza, Ch. Comninellis, N. Vatistas, J. Electrochem. Soc. 148 (2001) D78.
[39] H. Kuramitz, Y. Nakata, M. Kawasaki, S. Tanaka, Chemosphere 45 (2001) 37.
[40] H. Kuramitz, J. Saitoh, T. Hattori, S. Tanaka, Water Res. 36 (2002) 3323.
[41] H. Kuramitz, M. Matsushita, S. Tanaka, Water Res. 38 (2004) 2331.
[42] M.H. Zareie, B.K. Körbahti, A. Tanyolac, J. Hazard. Mater. B87 (2001) 199.
[43] J.C. Grigger, H.C. Miller, F.D. Loomis, J. Electrochem. Soc. 105 (1958) 100.
[44] S. Lormeau, M.H. Mannebach, M. Chemla, Electrochim. Acta 24 (1979) 823.
[45] N. Munichandraiah, J. Appl. Electrochem. 22 (1992) 825.
[46] G.P. Vercesi, J.Y. Salamin, Ch. Comninellis, Electrochim. Acta 36 (1991) 991.
[47] Ch. Comninellis, G.P. Vercesi, J. Appl. Electrochem. 21 (1991) 335.
[48] W.R. Grace & Co., Br. Pat. 1,156,309 (1969).
[49] J.D. Rodgers, W. Jedral, N.J. Bunce, Environ. Sci. Technol. 33 (1999) 1453.
[50] D. Wabner, C. Grambow, J. Electroanal. Chem. 195 (1985) 95.
[51] O. Simond, Ch. Comninellis, Electrochim. Acta 42 (1997) 2013.
[52] Ch. Comninellis, A. De Battisti, J. Chim. Phys. Phys.-Chim. Biol. 93 (1996) 673.
[53] S. Fierro, T. Nagel, H. Baltruschat, Ch. Comninellis, Electrochem. Commun. 9 (2007) 1969.
[54] S. Fierro, T. Nagel, H. Baltruschat, Ch. Comninellis, Electrochem. Solid-State Lett. 11 (2008) E20.
[55] W.R. Haag, C.D. Yao, Environ. Sci. Technol. 26 (1992) 1005.
[56] R.G. Zepp, B.C. Faust, J. Hoigné, Environ. Sci. Technol. 26 (1992) 313.
[57] Y. Sun, J.J. Pignatello, Environ. Sci. Technol. 27 (1993) 304.
[58] D. Fino, C. Carlesi Jara, G. Saracco, V. Specchia, P. Spinelli, J. Appl. Electrochem. 35 (2005) 405.
[59] M. Ferreira, H. Valera, R.M. Torresi, G. Tremiliosi-Filho, Electrochim. Acta 52 (2006) 434.
[60] X.-M. Wang, J.-M. Hu, J.-Q. Zhang, C.-N. Cao, Electrochim. Acta 53 (2008) 3386.
[61] N. Belhadj Tahar, A. Savall, Submitted to Electrochim. Acta, submitted for publication.
[62] M. Ueda, A. Watanabe, T. Kameyama, Y. Matsumoto, M. Sekimoto, T. Shimamune, J. Appl. Electrochem. 25 (1995) 817.